

PAPER • OPEN ACCESS

## Evaluation of the Temperature Distribution and Structural Deformation of the Car Dashboard Subjected to Direct Sunlight

To cite this article: A Yudianto *et al* 2019 *J. Phys.: Conf. Ser.* **1273** 012076

View the [article online](#) for updates and enhancements.



**IOP | ebooks™**

Bringing together innovative digital publishing with leading authors from the global scientific community.

Start exploring the collection—download the first chapter of every title for free.

# Evaluation of the Temperature Distribution and Structural Deformation of the Car Dashboard Subjected to Direct Sunlight

A Yudianto<sup>1</sup>, Saeid Ghafari<sup>2</sup>, Pierre Huet<sup>3</sup>, Muhkamad Wakid<sup>4</sup>

<sup>1,2,3</sup>Politecnico di Torino, Corso Duca degli Abruzzi, 24 - 10129 Turin, Italy

<sup>4</sup>Yogyakarta State University, Colombo Street 1, Yogyakarta 55281, Indonesia

E-mail: s250659@studenti.polito.it

**Abstract.** A situation in which the car is directly parked under the sunlight needs to be considered as one of unavoidable operating conditions. The thermal phenomenon perceived by car dashboard might affect its functionality. The biomechanical function of the dashboard focused on the thermo-structural evaluation due to the direct sunlight was numerically simulated and investigated in this work. Polypropylene was chosen as the main dashboard material. The aims are to evaluate the temperature distribution, stress distribution and structural deformation of a car dashboard subjected to direct sunlight and due to the outside air goes inside the passenger compartment through an air duct. The material yields a small temperature gradient due to both direct sunlight and air flow through the air duct. By imposing 400 W/m<sup>2</sup> heat flux on the dashboard surface, the stress distribution mainly occurs in the part of the applied constraints and the air duct placement, which has maximum value 19.56 MPa. The displacement of the dashboard is 0.0357 mm which is chiefly experienced by the front-centre part of the dashboard surface.

## 1. Introduction

The two main functions of the car dashboard in a car are aesthetic function and safety function. Since the dashboard is noticed immediately after opening the door and entering the car, it becomes the key element in the aesthetic judgement which is important in determining the rating of the vehicle. In the active safety aspect, dashboard acts as the element to distribute the air on the windshield and on the glass front door and. Thus, it is possible to acquire the more visibility through the appropriate apertures due to defroster or demister which are occurs on the dashboard. In terms of passive safety aspect, the requirements of the biomechanical performance of the dashboard must be respected [7]. Several operating conditions of the car should also be considered to be one of the main factors to design the proper characteristic of the dashboard. During a parking condition, for instance, it is quite frequently that the car is imposed directly by the sunlight. Since the windshield has considerable slope



angle, the sunlight imposed on it could be widely spread to the dashboard which is positioned exactly below the windshield. The thermal consideration becomes important in this case.

Several previous publications devoted in the understanding the characteristic of thermal deformation and car dashboard have been conducted by numerous researchers. Lee et al [1] analysed the thermal deformation and residual stress in automotive muffler. It results that the high tensile stress is produced in the region near the weld. Nabatilan et al [2] investigated the effect of driving experience on visual behaviour and driving performance under different driving conditions. It gives the importance of the present of the dashboard in a car due to more than 36% of novice drivers fixated more on dashboard area compared to other parts inside the driver compartment. Mantovani et al [3] studied the influence of manufacturing constraints on the topology optimization of an automotive dashboard. It is said that the manufacturing constraints strongly influence the design process of the component, the final shape, mass, and the stiffness of the dashboard. Belloti et al [4] designed configurable automotive dashboards on liquid crystal displays. An efficient exploitation of the visual space of the instruments cluster is deeply explained.

The distinct aspect of of this study is that it mainly investigates the thermo-structural analysis of the dashboard. The utilization of Hyperworks platform to simulate and approximate the phenomenon becomes preferable choice. However, the finite element method has received considerable attention in both engineering education and in industry sector as the solution for the complex industrial problems. It gives a piecewise approximation to the governing equations so that a solution domain can be modelled or approximated analytically by replacing the model with an assemblage of discrete elements. Since this discrete element can be put in a variety of ways, it can be utilized to represent exceedingly complex shapes [9]. The efficiency and the financial aspects make the finite element method a better solution to approximate the considered phenomena. Moreover, analysis by means of numerical investigation software greatly reduces the need for costly physical testing or performing prototyping. The aims of this study are to evaluate the temperature distribution, stress distribution and structural deformation including the displacement of the dashboard subjected to direct sunlight. The temperature distribution due to the temperature gradient between the outside temperature and cockpit temperature through the air duct is also to be considered.

## **2. Numerical Analysis Method**

### *2.1. Geometrical modelling of the dashboard*

The dashboard assembly consists of two main parts which are the main dashboard surface and the air duct. The main dashboard which is imposed by the sunlight that flows through the front windshield affects the structure. The conduction heat analysis becomes the best option to study this phenomenon. On the other hand, the air duct is designed in such a way so that the fresh air is able to enter into the cockpit. The thermal due to the direct sunlight and the heat transfer due to the air flow into the cockpit become the investigated phenomena in this study. The geometry of the model was modelled and then imported into Hyperworks platform to perform the analysis. The main dimension of the model is 1417 mm in the overall length, 590 mm in the overall width and 491 mm in the overall height. The shell element becomes the best choice considering the shape and the dimension of the model. The thickness is equally distributed which has the value of 2.5 mm. The mix between quads and trias mesh was generated with the element size of 10 mm. The element checking was performed in order to ensure the accuracy of the simulation. Figure 1 shows the mesh of both the air duct and the

main dashboard component. It can be seen that the element size is reasonably representative to yields the accurate approximation of the results. The proportion of the mesh element is equally distributed due to the fact that, in this study, it is important to highlight every detail of the results that is distributed in all parts of the model.

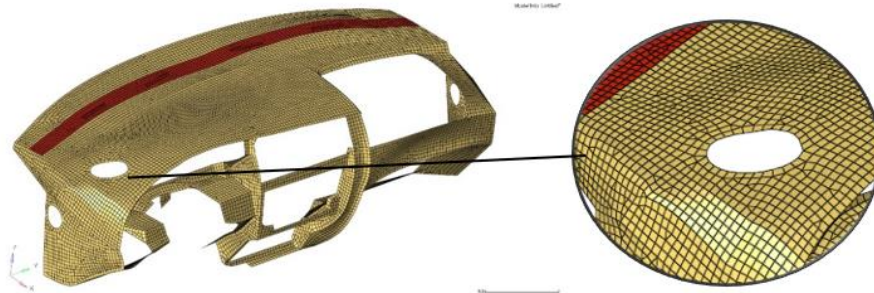


**Figure 1.** Mesh of the elements

### 2.2. Material properties

Polypropylene is one of the most common materials that is utilized for car dashboard material. It is thermoplastic polymer that a saturated addition polymer is made from the monomer propylene. It is rugged and unusually resistant to many chemical solvents, bases and acids. The technology used is the injection moulding of thermoplastic materials, belonging to the family of Polyolefin (Polypropylene) by adding mineral (talc) and elastometric filters of mixture between ABS and Polycarbonate [7]. In this study, Polypropylene material is chosen and the properties such as the young's modulus, poisson ratio, material density, thermal expansion coefficient, thermal conductivity and heat transfer coefficient are explained in Table 1.

**Table 1.** Propylene material properties.

	Value	Unit
Young's modulus	1800	MPa
Poisson ratio	0.45	-
Material density	946	kg/m <sup>3</sup>
Thermal expansion coefficient	150x10 <sup>-6</sup>	1/°C
Thermal conductivity	0.16	W/(m°C)
Heat transfer coefficient	25.4	W/(m <sup>2</sup> °C)

### 2.3. Boundary Condition

It is assumed that the internal cockpit temperature is 60°C. Two single-point constraints are set in the point in which the dashboard is supported into the body of the car. The rigid web elements are created in the constraints to ensure that the forces are equally distributed into the dashboard mounting. The outside temperature is chosen so that it can be simulated flowing through the air duct and goes inside the cockpit. The points along the air duct is set as rigid as well, taking into consideration that it is the attachment point of the car dashboard into the main body of the car. Furthermore, the heat flux 400 W/m<sup>2</sup> as the representative of the direct sunlight is imposed directly in the area showed in point 3 in Figure 2.

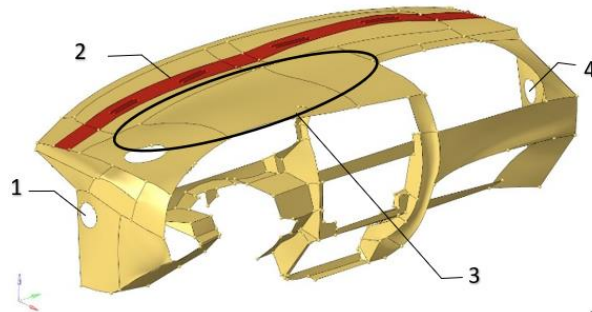


**Figure 2.** The applied constraints (1 and 4), the air duct (2), the area of imposed sunlight (3)

### 3. Governing Equations

#### 3.1. Thermal Analysis

The determination of temperature distribution in a medium which can be solid, liquid, gas or combination of phases is the main objective of conduction analysis. Therefore, it is to understand the temperature in medium as a function of space at steady state. This becomes important due, in the end, the determination of the structural integrity via a determination of thermal stresses and temperature distribution, the optimization of the thickness of the material can then be determined [5]. According to *Fourier's law*, the rate of heat conducted ( $\dot{Q}$ ) through a body is proportional to the cross-sectional area ( $A$ ) and temperature gradient ( $\partial T/\partial x$ ) in the body [6], which can be expressed as

$$\dot{Q}_x \propto -A \frac{\partial T}{\partial x} \quad (1)$$

$$\dot{Q}_x = -kA \frac{\partial T}{\partial x} \quad (2)$$

where the constant of proportional  $k$  is thermal conductivity of the body material.

#### 3.2. Mechanical Analysis

The maximum distortion energy criterion indicates that material failure occurs when the distortion energy of a component reaches the energy for yielding [8]. To ensure that component is in the safe region, the following relation has to be met

$$\sigma_1^2 - \sigma_1\sigma_2 - \sigma_2^2 < \sigma_{yield}^2 \quad (3)$$

The stress field of the model that is used to draw the theoretical closed-form stress solution can be expressed by *Von Mises* yield criterion

$$\sigma_{von\ mises} = \sqrt{\frac{1}{2}[(\sigma_1 - \sigma_2)^2 + (\sigma_2 - \sigma_3)^2 + (\sigma_3 - \sigma_1)^2]} \quad (4)$$

where  $\sigma_1, \sigma_2, \sigma_3$  are the principle stresses.

## 4. Simulation Result and Discussion

### 4.1. Temperature Evaluation

The subcase analysis of the heat transfers due to the air flowing through the air duct is depicted in the Figure 3. The temperature differences between the initial temperature of the air entering the air duct and the temperature inside the cockpit creates temperature gradient in the dashboard component. It is worth to mention that due to  $10^{\circ}\text{C}$  of air entering through the air duct and  $60^{\circ}\text{C}$  of internal cockpit temperature, the length of temperature gradient is approximately equal to the length of the mesh element which is 10 mm. It is equally distributed along the length of the outer part of the air duct which is adjacent to the dashboard component. This heat transfer does not affect much the temperature distribution except this location. However, this behaviour is considered good for the component, since the temperature distribution may cause the higher structural deformation which is explained in the next point.

In case of the direct sunlight imposed to the dashboard (Figure 4), the subcase of the heat distribution due to conduction is more appropriate to be used to analyse the phenomena. Two main temperature distributions occur in the outside area close to the imposed sunlight and in the outside area of the air duct. The  $400\text{ W/m}^2$  of imposed heat flux generates approximately  $76.39^{\circ}\text{C}$  of temperature in the dashboard and it propagates to the dashboard surface, so that the main area of the dashboard has approximate temperature between  $54.26^{\circ}\text{C}$  and  $61.63^{\circ}\text{C}$ . In the outer area of the air duct, considering only the direct sunlight generates the temperature distribution between  $24.75^{\circ}\text{C}$ –  $39.50^{\circ}\text{C}$ .

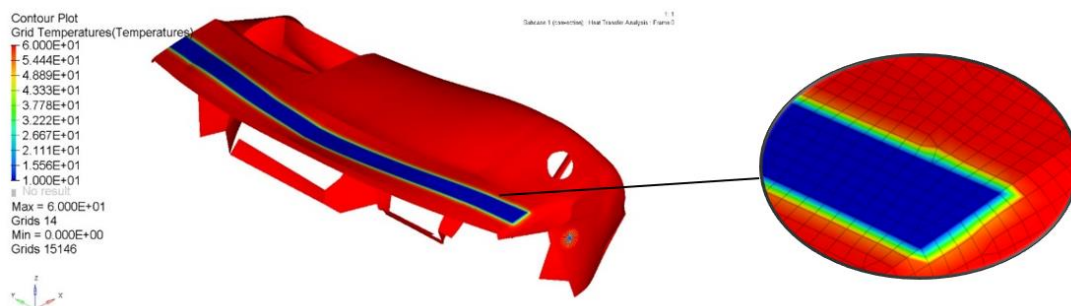


**Figure 3.** Temperature distribution due to the direct sunlight

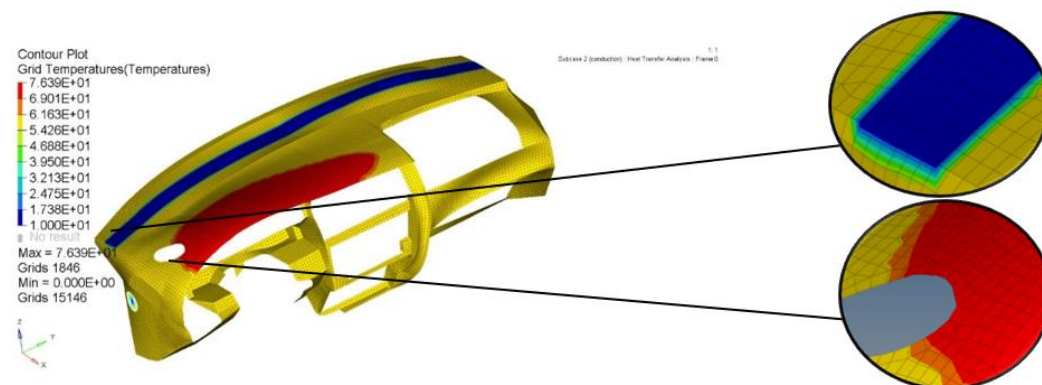


**Figure 4.** Temperature distribution due to the air flowing through the air duct

4.2. Stress Distribution

The residual stress is calculated from the temperature distribution determined by thermal analysis. The structural deformation is caused by extremely non-uniform temperature distribution on the model. The representation of the stress distribution in all part of the dashboard surface is clearly compared in Figure 5. The *Von Mises* stress distribution is investigated to determine the overall result of the residual stress state. The numerical prediction of the stress distribution is also investigated in three directions. The simulation results in three directions are respectively shown in Figure 5 (b) (c) and (d). The  $\pm$  sign indicates the compression stress and tensile stress experienced by the dashboard. As depicted in the *Von Mises* stress distribution, the maximum stress undergone by model is in the order of 19.56 MPa. However, based on the standard material properties, the average tensile strength of Polypropylene Homopol is 33 MPa and Polypropylene Copolym is 25 MPa. In this case, by having 400 W/m<sup>2</sup> of heat flux, the stress does not exceed the value of tensile strength of the material. Therefore, it does not undergo the permanent deformation. Further investigation of the results, the maximum stress is indicated in the main constrain zones and in the area close to the air duct. It can also be seen that the area in which the part of the dashboard, where several electronic devices are normally placed, indicated with several small and complex shapes in the part of the dashboard does not experience excessive stress.

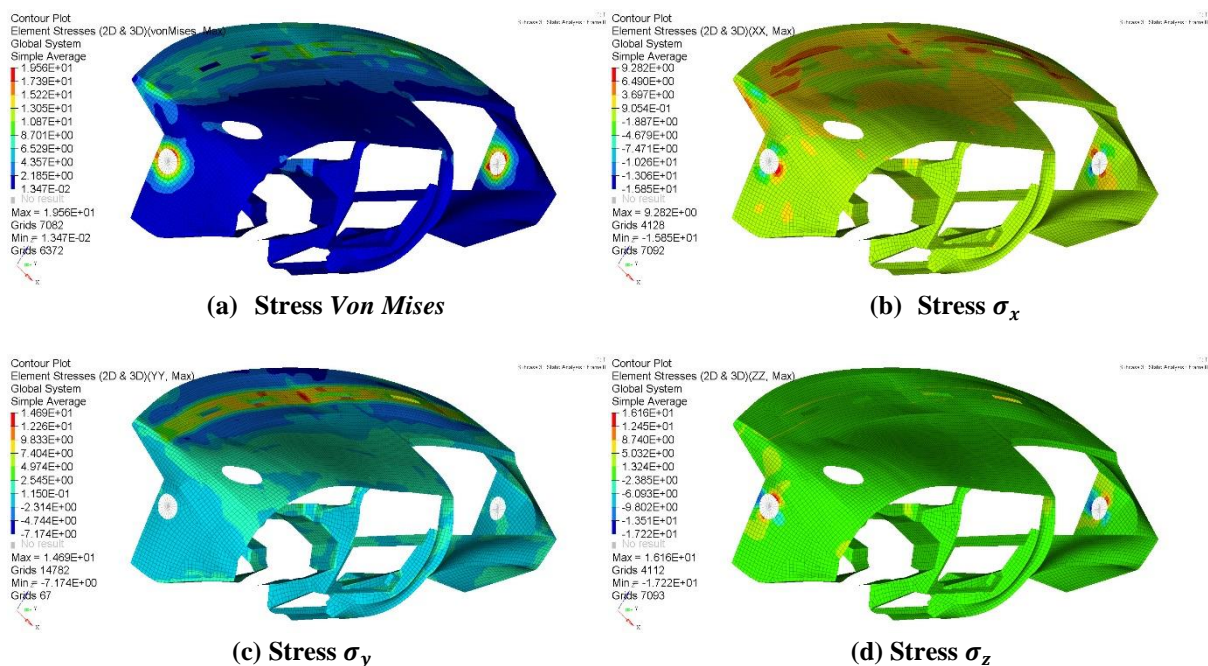


Figure 5. Stress distribution *Von Mises*,  $\sigma_x$ ,  $\sigma_y$ ,  $\sigma_z$

In the *Von Mises* stress, the maximum stress is in the order of magnitude 19.56 MPa. Stress in  $x$  direction has the maximum compression stress 9.28 MPa and tensile stress is approximately 15.85 MPa. For the stress in  $y$  direction, the highest stress occurs in the area of the air duct with 14.69 MPa of compression stress and 7.17 MPa of tensile stress. Considering the stress in  $z$  direction, the critical part of the dashboard is in the place in which the rigid spider constraints are applied. It experiences 16.16 MPa of compression stress and 17.22 MPa tensile stress. Therefore, considering the overall result, the

critical section of the dashboard due to the stress distribution occurs mainly in the area of the air duct and in the constrain where the main mountings are applied.

#### 4.3. Displacement

The thermal deformation of the dashboard has been calculated and the results are depicted in Figure 6 (a), (b), (c), and (d). Considering the inner cockpit temperature and the heat flux imposed to the dashboard, the overall displacement is in the order of 0.035 mm which mainly occur in the centre-front part of the dashboard (Figure 6 (a)). The place in which constraints are applied in both right and left side of the dashboard is nearly does not have displacement, represented in the blue colour in the Figure 6 (a). Investigating the displacement in  $x$  direction, the maximum displacement of 0.00461 mm is experienced by the dashboard in the side towards to the occupants. The graphical representation of the distribution of the results can be clearly seen in the Figure 6 (b). Figure 6 (c) shows the deformation in  $y$  direction that mainly occurs in the right part of the dashboard with respect to direction perceived from the driver. It has maximum displacement of 0.00641 mm. Figure 6 (c) represents the displacement in  $z$  direction. The result in this direction is very similar with the overall displacement (Figure 6 (a)). The main deformation occurs in the front centre part of the dashboard which has value 0.0356 mm. The  $\pm$  sign indicates the direction of the displacement with respect to each reference system.

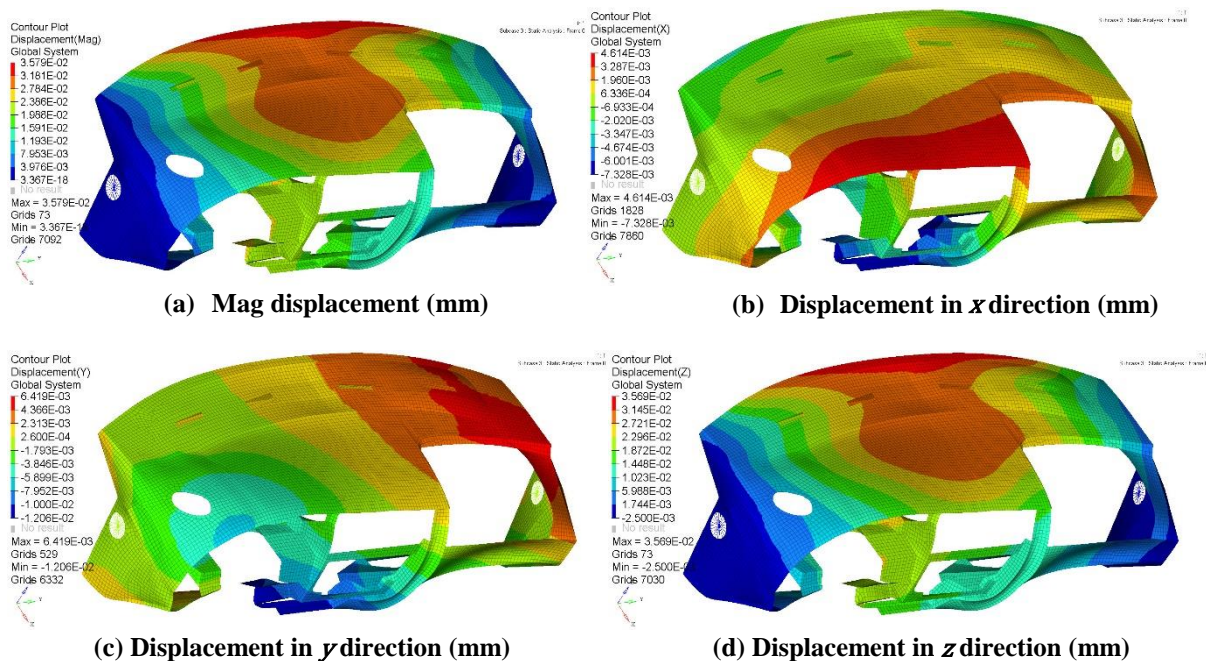


**Figure 6.** Overall displacement, displacement in  $x$ ,  $y$ ,  $z$  direction

The deformation of the model becomes important due to the fact that it has effects in the assembly and might cause the vibration, unwanted noise or even structural failure if the displacement exceeds the limited value. Comparing all the results, it can be said that the deformation due to the thermal effect imposed by direct sunlight mainly occurs in the top part of the surface.

## 5. Conclusion

The 400 W/m<sup>2</sup> of heat flux in the part of dashboard surface simulates the direct sunlight imposed on it. By means of conduction, the temperature gradients are numerically calculated. The major part of the dashboard surface has temperature between 54.26 °C and 61.63 °C. However, small temperature gradient occurs in the outside area of the imposed heat flux and the vicinity of the part of the air duct. Due to the fresh air flowing through the air duct, the 10 °C of outside temperature and 60 °C of cockpit temperature results a temperature gradient as well. However, this temperature gradient has small range and the length is approximately 10 mm. By applying constraints in which the two main mountings of the dashboard are applied, the stress distribution by *Von Mises* approximation is distributed mainly in the area of rigid constraints and slight smaller in the area of air duct. The maximum value of overall stress distribution is in the order of 19.56 MPa which is close to the constraints. This is, however, still in the safe region due to the value is still below the tensile strength of the material. The maximum overall displacement 0.0357 mm occurs in the front-middle part of the dashboard. Future works are planned to identify the mechanical analysis of the dashboard due to vibration of both internal and external excitation and the analysis of the optimal placement of the dashboard mounting considering the stress distribution in severe condition.

## Acknowledgments

Authors are particularly grateful for the funding given by *Lembaga Pengelola Dana Pendidikan (LPDP)*. My special appreciations are extended to Prof Andrea Trivella and Alessandro Scattina for the explanation in conducting this work.

## 6. References

- [1] S H Lee, E S Kim, J Y Park, and J Choi 2018 *Numerical Analysis of Thermal Deformation and Residual Stress in Automotive Muffler by MIG Welding* Journal of Computational Design and Engineering 5 p 382 - 390
- [2] L B Nabatilan, F Aghazadeh, A D Nimbarte, C C Harvey, and S K Chowdhury 2012 *Effect of Driving Experience on Visual Behavior and Driving Performance under Different Driving Condition* Cogn Tech Work 14 p 355 - 363
- [3] S Mantovani, I L Presti, L Cavazzoni, and A Baldini 2017 *Influence of Manufacturing Constraints on the Topology Optimization of an Automotive Dashboard* Procedia Manufacturing 11 p 1700-1708
- [4] F bellotti, A D Gloria, A Poggi, L Andreone, S Domiani, and P Knoll 2014 *Designing Configurable Automotive Dashboards on Liquid Crystal Displays* Cogn Tech Work 6 p 247 - 265
- [5] P Nithiarasu, R W Lewis and K N Seetharamu 2016 *Fundamentals of the Finite Element Method for Heat and Mass Transfer: Second Edition* (United Kingdom: Wiley)
- [6] A K Tamrakar and D Harursampath 2016 *Acing the GATE Mechanical Engineering* (India: Wiley)
- [7] L Morello, L R Rossini, G Pia, and A Tonoli 2011 *The Automotive Body Volume I: Components Design* (New York: Springer)
- [8] Amir Javidinejad 2015 *Essential of Mechanical Stress Analysis* (Boca Raton: CRC Press)
- [9] E A Baskharone 2014 *The Finite Element Method with heat Transfer and Fluid Mechanics Applications* (New York: Cambridge University Press)
- [10] A Scattina and A Trivella 2018 *Numerical Modelling and Simulation Lecture Notes* Politecnico di Torino